

## Size-dependent resistivity of nanometric copper wires

H. Marom,<sup>1,\*</sup> J. Mullin,<sup>2</sup> and M. Eizenberg<sup>1</sup>

<sup>1</sup>*Department of Materials Engineering, Technion—Israel Institute of Technology, 32000 Haifa, Israel*

<sup>2</sup>*Tower Semiconductor Ltd., 23105 P.O. Box 619, Migdal Haemek, Israel*

(Received 15 March 2006; published 11 July 2006)

Higher electrical resistivity is observed in metals when dimensions approach the mean free path of the electrons. The effects of electron scattering at surfaces and at grain boundaries are then becoming substantial. This issue has been extensively studied on thin films but rarely on wires, where both small dimensions (width and height) influence the resistivity increase. In this study, copper wires having variable width and height down to 100 nm are investigated. An alternative approach is suggested in which the resistivity of such wires at different temperatures is compared to that of films having thickness that is equal to the height of the wires. The main outcome is a reliable model that overcomes the well-known difficulty of separating the contribution of surfaces to the resistivity from that of grain boundaries. It is shown that when both width and height of the wire are larger than one third of the mean free path, its resistivity exhibits a filmlike behavior with a separate contribution to the resistivity of each small dimension. The scattering of electrons at the surfaces of the investigated wires was best described by a zero specularly parameter, indicating the importance of this effect for the resistivity increase in small wires.

DOI: [10.1103/PhysRevB.74.045411](https://doi.org/10.1103/PhysRevB.74.045411)

PACS number(s): 73.63.-b, 73.50.-h, 73.50.Bk

### I. INTRODUCTION

Materials with nanometric dimensions exhibit higher electrical resistivity due to additional scattering centers for the conduction electrons, mainly from surfaces and grain boundaries. Higher resistivity is observed when at least one of the material's dimensions approaches the mean free path of the electrons. The collisions of the electrons with surfaces and grain boundaries are then becoming substantial in comparison to their collisions with other lattice imperfections. This issue has been a topic for extensive studies in the last several decades. Most noteworthy are the pioneering works of Fuchs,<sup>1</sup> who attributed the resistivity increase to the diffuse scattering of the electrons at the surfaces, and of Mayadas and Shatzkes<sup>2</sup> who realized the importance of electron scatterings at the grain boundaries. Each of these theories suggested a phenomenological parameter with which the resistivity increase can be quantified: the specularly parameter of the surfaces ( $p$ ) in the first case and the grain boundary reflection coefficient ( $R$ ) in the second. These parameters enable the testing of these theories against experimental data and the verification of their validity. Extensive work has been made in this regard on thin films with variable thickness, as, for example, in some recent studies on copper,<sup>3-5</sup> a material which draws special interest as an interconnecting metal in the continuously shrinking dimensions of integrated circuits.

When wires (and not films) are concerned, a different picture is revealed. Only very little experimental data is available, lacking especially in the highly interesting case of wires with two small dimensions. For rectangular wires, it means that both width and height are small in comparison to the mean free path of the electrons. The surface-induced resistivity is then no longer filmlike, but rather exhibits a more complicated behavior on which this study is focused. The few previous attempts to tackle this problem analyzed wires with constant height and only variable width<sup>6,7</sup> or such that were measured only at room temperature.<sup>8</sup> We use sets of

wires when both width and height are varying. Furthermore, the resistivity measurements are carried out at both room and liquid nitrogen temperatures. This enables us to analyze an alternative approach in which the resistivity of each wire (with known width and height) is compared to that of a film with identical height (thickness). The main outcome is a more reliable model that succeeds in separating the contributions to the resistivity of surfaces versus grain boundaries. This is an essential step towards better understanding of each effect. We chose copper wires as our model system due to their technological importance as interconnects in integrated circuits.

### II. EXPERIMENTAL

Copper wires of rectangular profile were embedded inside SiO<sub>2</sub> layers grown on a silicon substrate. Different SiO<sub>2</sub> thicknesses were chosen to control the depth (height) of the trenches that were later etched inside the SiO<sub>2</sub> layer. For each height, the same lithography mask was used to create trenches of different widths, together with a Van der Pauw structure for a film having the same height as the trenches. The resulting structures were lined with a thin tantalum layer and were then electrochemically filled with copper. After removal of the excess copper by chemical mechanical polishing, the wires (and films) were covered with a silicon oxynitride passivation layer. In this way, an array of wires with different dimensions was obtained, having width in the range of 100 to 200 nm, height in the range of 150 to 300 nm, and a constant length of 100  $\mu$ m. Each set of wires with variable width was accompanied by a corresponding film having the same height (thickness).

The resulting structures were imaged using a high-resolution scanning electron microscope. Figure 1 shows a top view of the Van der Pauw structure containing the film and two of the neighboring wires. The surrounding pads used for the resistivity measurements can also be seen. Figure 2

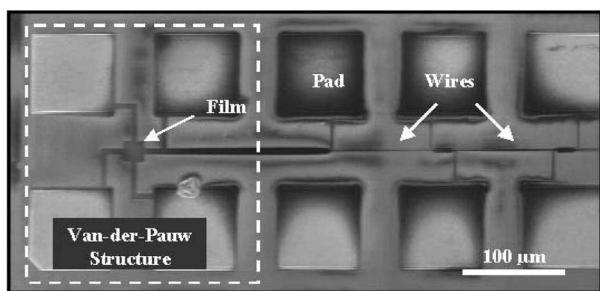


FIG. 1. Scanning electron microscope top view image of the Van der Pauw structure containing the film and two of the neighboring wires. The surrounding pads were used for the resistivity measurements in a standard four terminal configuration.

shows a series of cross-sectional images taken for one set of wires having a constant height (156 nm in this case) and a variable width. From such images the dimensions of copper in each wire can be determined. Three wires are shown for each width to demonstrate the good uniformity of the process, resulting in dimension and resistivity spans of less than 5%. The resistance of the wires was measured in a standard four-terminal configuration using currents of up to 10 μA to

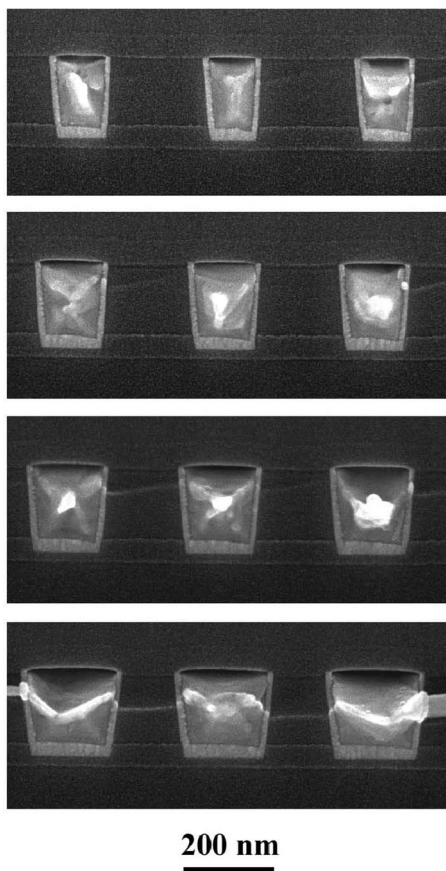


FIG. 2. Scanning electron microscope cross-section images of one set of wires having constant height (156 nm in this case) and variable width. Three copper wires are shown for each width, surrounded by the peripheral tantalum layer. Nonuniformity in the copper appearance is due to the plastic deformation caused by the cut made for preparing the cross-section samples.

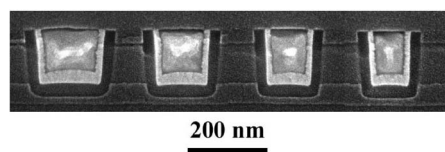


FIG. 3. Scanning electron microscope cross-section images of a set of wires where its trenches were lined with a SiO<sub>2</sub> layer before tantalum and copper filling. Smaller wires were thus obtained, about 100 nm in height and down to 80 nm in width. The original trenches before deposition of the extra SiO<sub>2</sub> layer can also be seen.

avoid heating. Resistivity was calculated from the resistance and the measured dimensions of the copper, neglecting the tantalum since its resistivity is at least one order of magnitude higher than that of the copper. After measurements at room temperature, all structures were dipped in liquid nitrogen and remeasured for their resistivity at this temperature.

One set of wires was prepared in a different way to further reduce its dimensions. After etching of the trenches, they were first lined with a SiO<sub>2</sub> layer and only then the regular process of tantalum and copper filling was continued. Smaller wires were obtained this way, about 100 nm high and down to 80 nm wide, as shown in Fig. 3. The original trenches before the addition of the extra SiO<sub>2</sub> layer can be clearly seen.

### III. MODELING

#### A. Surface-induced resistivity of a rectangular wire

Fuchs<sup>1</sup> developed the following expression for the resistivity of a thin film ( $\rho_f$ ) that is higher than that of a bulk material ( $\rho_B$ ) due to the diffuse scattering of electrons at the surfaces,

$$\frac{\rho_B}{\rho_f} = 1 - \frac{3\lambda}{2h}(1-p) \int_0^{\pi/2} \cos \theta \times \sin^3 \theta \frac{1 - \exp\left(-\frac{h}{\lambda \cos \theta}\right)}{1 - p \exp\left(-\frac{h}{\lambda \cos \theta}\right)} d\theta, \quad (1)$$

where  $h$  is the film thickness,  $\lambda$  is the mean free path of the electrons in a bulk material, and  $p$  is the specularity parameter, representing the fraction of specular (versus diffuse) scatterings at the surfaces.

A similar approach can be used to analyze the resistivity of a wire due to the diffuse scatterings at its walls, as implemented by MacDonald and Sarginson<sup>9</sup> for square wires and by Dingle<sup>10</sup> for circular ones. It is possible in principle to extend this approach for rectangular wires, but this is expected to result in complicated expressions that may not be simplified for calculation. Chambers<sup>11</sup> developed an alternative method, based on kinetic theory arguments, with which the resistivity of a wire with an arbitrary shape can be calculated. Authors who implemented this approach for rectan-

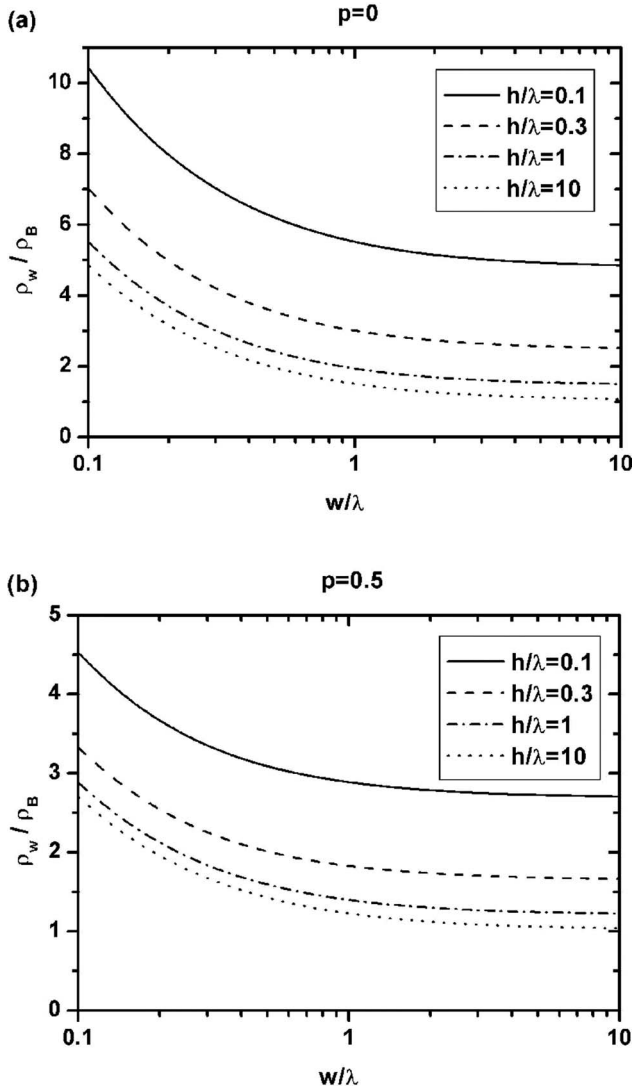


FIG. 4. Calculated resistivities of rectangular wires taking into account the effect of electron scattering at the wire's walls: (a) fully diffuse scattering and (b) partially diffuse scattering with specularity parameter of  $p=0.5$ . Dimensions are shown with respect to the mean free path of the electrons for continuous range of widths ( $0.1 \leq w/\lambda \leq 10$ ) and several representing heights ( $h/\lambda=0.1, 0.3, 1, 10$ ). The effect of two small dimensions is demonstrated.

gular wires<sup>6,7</sup> have reached different results that we find incorrect in one case<sup>6</sup> and inaccurate (probably due to typographical error) in the other.<sup>7</sup> We therefore elaborate on deriving our expression in the Appendix.

For the case of fully diffuse scattering at the wire's walls ( $p=0$ ), we obtained the following expression for the resistivity ( $\rho_w$ ):

$$\frac{\rho_w}{\rho_B} = 1 - \frac{3}{2\pi h w} (I_{DA} + I_{AB}), \quad (2)$$

where  $I_{DA}$  and  $I_{AB}$  are the following integrals:

$$I_{DA} = \int_0^w dx \int_0^h dy \int_{\arctan[(y-h)/x]}^{\arctan(y/x)} d\phi \int_0^\pi d\theta \sin \theta \cos^2 \theta \times \exp\left(-\frac{x}{\lambda \sin \theta \cos \phi}\right), \quad (3)$$

$$I_{AB} = \int_0^w dx \int_0^h dy \int_{\arctan[(x-w)/y]}^{\arctan(x/y)} d\phi \int_0^\pi d\theta \sin \theta \cos^2 \theta \times \exp\left(-\frac{y}{\lambda \sin \theta \cos \phi}\right). \quad (4)$$

We find the result in Ref. 6 incorrect because both the function to integrate and the  $\phi$  limits of integration must depend on the  $x$  and  $y$  coordinates (numerical calculations also yielded different results). In comparison to Ref. 7, our  $\cos^2 \theta$  is replaced there by  $\cos^2 \phi$ , probably due to a typographical error.

The above expressions contain fourth-order integrals that are relatively difficult for numerical calculations. We have managed to simplify and reduce them to first- and second-order integrals that are much easier to calculate (using different mathematical manipulations that involved Kaplan's generalization for the Leibniz integral rule, integrations by parts and changes in the order of integration). The following result that is mathematically identical to the former one is obtained:

$$\frac{\rho_w}{\rho_B} = 1 - S_1 - S_2 - S_3, \quad (5)$$

where

$$S_1 = \frac{3\lambda}{8h} \left[ 1 - \frac{8}{\pi} \int_0^\pi d\theta \sin^2 \theta \cos^2 \theta \int_0^{\arctan(w/h)} d\phi \cos \phi \times \exp\left(-\frac{h}{\lambda \sin \theta \cos \phi}\right) \right], \quad (6)$$

$$S_2 = \frac{3\lambda}{8w} \left[ 1 - \frac{8}{\pi} \int_0^\pi d\theta \sin^2 \theta \cos^2 \theta \int_0^{\arctan(h/w)} d\phi \cos \phi \times \exp\left(-\frac{w}{\lambda \sin \theta \cos \phi}\right) \right], \quad (7)$$

$$S_3 = \frac{4}{5\pi h w} \left\{ -1 + \frac{15}{4} \int_0^\pi d\theta \sin^3 \theta \cos^2 \theta \left[ \exp\left(-\frac{h}{\lambda \sin \theta}\right) + \exp\left(-\frac{w}{\lambda \sin \theta}\right) - \exp\left(-\frac{\sqrt{w^2 + h^2}}{\lambda \sin \theta}\right) \right] \right\}. \quad (8)$$

When either  $h$  or  $w$  approaches infinity, the result converges to that of Fuchs for thin films. The resistivity of the wire is affected not only by the separate contributions of each small dimension (filmlike behavior) but also by the interaction between them. Using these expressions, the resistivity of different wires was calculated for the case of fully diffuse scattering ( $p=0$ ) as shown in Fig. 4(a). Dimensions

are shown with respect to the mean free path of the electrons, for a continuous range of widths ( $0.1 \leq w/\lambda \leq 10$ ) and several representative heights ( $h/\lambda = 0.1, 0.3, 1, 10$ ). The effect of two small dimensions can be very strong, as demonstrated, for example, in the case of the smallest calculated wire with normalized height and width of  $h/\lambda = 0.1$  and  $w/\lambda = 0.1$  respectively. A resistivity value 10.4 times larger than the bulk value is then obtained, in comparison to only 4.8 times larger for a film with the same thickness.

To describe real systems, a nonzero specularly parameter ( $p \neq 0$ ) should be considered. As shown by Chambers,<sup>11</sup> the resistivity in this case can be expressed in terms of that with zero specularly parameter by the following series expansion:

$$\left(\frac{\rho_B}{\rho_w}\right)_{p,\lambda} = (1-p)^2 \sum_{n=1}^{\infty} n p^{n-1} \left(\frac{\rho_B}{\rho_w}\right)_{0,\lambda/n}, \quad (9)$$

where  $(\rho_B/\rho_w)_{p,\lambda}$  is the bulk to wire resistivity ratio in the case of specularly parameter  $p$  and mean free path  $\lambda$  and  $(\rho_B/\rho_w)_{0,\lambda/n}$  is this ratio in the case of zero specularly parameter and mean free path  $\lambda/n$ . The higher  $p$  is, the lower the resistivity, as demonstrated in Fig. 4(b) for the same wires calculated in Fig. 4(a), but with a specularly parameter of  $p=0.5$ .

### B. Grain boundary-induced resistivity of a rectangular wire

The effect of grain boundaries on the resistivity of thin films is commonly explained by the theory of Mayadas and Shatzkes.<sup>2</sup> According to this theory, the resistivity of a thin film ( $\rho_f$ ) that is higher than that of a bulk material ( $\rho_B$ ) only due to the scattering of electrons at the grain boundaries is given by

$$\frac{\rho_B}{\rho_f} = 1 - \frac{3}{2}\alpha + 3\alpha^2 - 3\alpha^3 \ln\left(1 + \frac{1}{\alpha}\right), \quad (10)$$

where  $\alpha$  is a parameter defined by

$$\alpha = \frac{\lambda}{D} \frac{R}{1-R}, \quad (11)$$

$\lambda$  is the mean free path of the electrons,  $D$  is the mean grain size, and  $R$  is the grain boundary reflection coefficient, representing the fraction of electrons reflected backward at scattering from each grain boundary.

Unlike the case of surface-induced resistivity, here it is tempting to use the film model also for wires, since only grain boundaries that are perpendicular to the direction of the current are being considered anyway. Such an approach is valid provided the wires have columnar grains structure (as in films), or at least semicolumnar, with grains not necessarily extending from bottom to top, but having boundaries perpendicular to the main axis of the wire. Experimental evidence that this is the case in our study is given in Fig. 5. All grain boundaries clearly fit this description, justifying the use of the film model also for wires. A difference between films and wires may still exist in the average size of the grains that may be limited in wires not only by their height but also by their width.

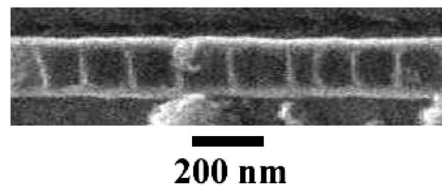


FIG. 5. Top view of a scanning electron microscope image of a wire with approximately a square profile of 150 nm. Grain structure seems to be columnar with grain boundaries that are clearly perpendicular to the length of the wire (the direction of current).

### C. The combined resistivity of a rectangular wire

The influence of both surfaces and grain boundaries needs to be considered when we want to analyze real wires. Assuming each mechanism can be described by an independent relaxation time, Matthiessen's rule can be applied and the contributions to the resistivity can be added. Taking into account the contributions of background (bulk) scattering ( $\rho_B$ ), surface scattering ( $\rho_s^*$ ), and grain boundary scattering ( $\rho_g^*$ ), the total resistivity ( $\rho$ ) can be expressed as

$$\rho = \rho_B + \rho_s^* + \rho_g^*. \quad (12)$$

It is more convenient to replace the excess resistivity due to each size-dependent effect by the total resistivity resulting from this effect. Denoting by  $\rho_s$ , the resistivity of a film or wire taking into account only the surface effect ( $\rho_s = \rho_B + \rho_s^*$ ), and by  $\rho_g$  its resistivity taking into account only the grain boundaries effect ( $\rho_g = \rho_B + \rho_g^*$ ), the total resistivity can be written as

$$\rho = \rho_g + \rho_s - \rho_B. \quad (13)$$

The advantage of this form is that expressions for  $\rho_s$  and  $\rho_g$  were already given in other notations:  $\rho_s$  is the same as  $\rho_f$  in Eq. (1) for films or as  $\rho_w$  in Eqs. (5) and (9) for wires.  $\rho_g$  is identical to  $\rho_f$  in Eq. (10) for films, which holds also for wires. Although Matthiessen's rule is not valid for this combined case of scattering mechanisms (background, surfaces, and grain boundaries), calculations show that the above expression gives a very good approximation in comparison to the accurate treatment made by Mayadas and Shatzkes for thin films. We will therefore use this approximation for both films and wires.

In principle, it is possible to fit experimental results to Eq. (13), with a minimal number of two free parameters that are needed ( $p$  for  $\rho_s$  and  $R$  for  $\rho_g$ ), provided the dimensions, the mean grain size, and the bulk properties ( $\lambda, \rho_B$ ) of the material are known. The problem with this approach is that different sets of  $p$  and  $R$  values, representing different contributions to the resistivity of surfaces and grain boundaries, can be fitted equally well, as we demonstrated in a previous work for thin films.<sup>12</sup> The same problem exists also for wires as shown in Fig. 6 using the results of Steinhogel *et al.*<sup>7</sup> for copper wires 230 nm in height and 40–800 nm in width. The authors best fitted their results to the values of  $p=0.6$  and  $R=0.50$ , assuming a certain mean grain size for each wire. As can be seen in the figure, extreme values of the specularly parameter, from fully diffuse surface scattering ( $p=0$ ) to

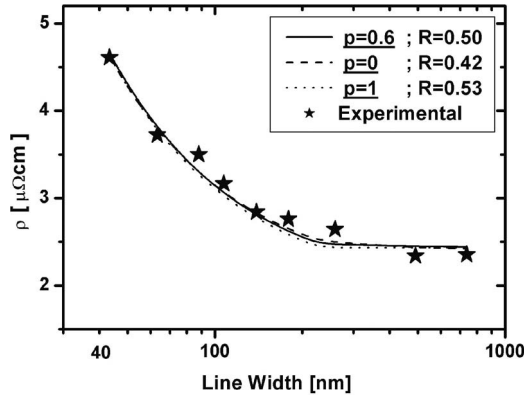


FIG. 6. Demonstrating the difficulty in extracting meaningful parameters of surface scattering versus grain boundary scattering from experimental results. Theoretical curves were fitted to the results of Steinhogel *et al.*<sup>7</sup> for the resistivity of copper wires 230 nm high and 40–800 nm wide. As can be seen, extreme values of specularly parameter, ranging from fully diffuse surface scattering ( $p=0$ ) to no influence of surface scattering at all ( $p=1$ ), can be fitted equally well (parameters in the first row are the original authors' choice).

no influence of surface scattering at all ( $p=1$ ), can be fitted equally well. In a more recent work,<sup>8</sup> the authors tried to set some limits on the range of these parameters, but a distinct separation between them remained a severe problem. Without such a distinction, there is no reliable way to test the theory and extract meaningful parameters. In particular, it is impossible to study the surface effect by itself, and analyze the difference in this effect between films and wires.

#### D. A new approach to study the resistivity of rectangular wires

To deal with the above-mentioned problem, we suggest an approach where the resistivity of the wire at different temperatures is compared to that of a film that its thickness is equal to the height of the wire. Since Eq. (13) is valid for both films and wires, we can write

$$\rho_f = (\rho_g)_f + (\rho_s)_f - \rho_B, \quad (14)$$

$$\rho_w = (\rho_g)_w + (\rho_s)_w - \rho_B. \quad (15)$$

The subscripts  $f$  and  $w$  denote whether a film or a wire is being considered. Subtracting one equation from the other yields

$$\rho_w - \rho_f = [(\rho_g)_w - (\rho_g)_f] + [(\rho_s)_w - (\rho_s)_f]. \quad (16)$$

The difference between the resistivity of the wire and that of the film can be expressed as the sum of the differences in their grain boundaries and in their surface-induced resistivities. We will choose such a film that its thickness is equal to the height of the wire. If only the vertical dimension determines the mean size of the grains, then both the film and the wire are expected to have the same component of grain boundaries induced resistivity. This is certainly a good assumption for wide wires, where the process of grain growth is not limited by their width and a columnar grain structure is

developed with grains extending from the bottom to the top surface. As explained by Thompson,<sup>13</sup> the mean grain size in this case is determined by the vertical dimension, so both film and wire would have the same value and hence the same grain boundaries induced resistivity. In such a case the difference  $[(\rho_g)_w - (\rho_g)_f]$  can be neglected and we can write

$$\rho_w - \rho_f = (\rho_s)_w - (\rho_s)_f. \quad (17)$$

Our experimental results show that neglecting the difference  $[(\rho_g)_w - (\rho_g)_f]$  is justified in our case also for narrow wires with widths that are smaller than the height, provided both dimensions are larger than 100 nm (see Sec. IV or further details). Equation (17) is therefore valid for all our wires. It means that the difference between the resistivity of the wire and that of the chosen film (with identical height) is equal to the difference in their surface-induced resistivity, which is just the effect we wanted to isolate. At room temperature, this difference is small because the dimensions are still large in comparison with the mean free path of the electrons (about 40 nm for copper). But lowering the temperature increases the mean free path, and should therefore emphasize the relative importance of the surface effect. The difference between the resistivities of the wire and the film could then be observed. We chose to work at liquid nitrogen temperature (77 K) when the mean free path of the copper electrons (about 300 nm) is much larger than the wire's dimensions.

Equation (17) can also be written as

$$\rho_w - \rho_f = \rho_B \left[ \frac{(\rho_s)_w}{\rho_B} - \frac{(\rho_s)_f}{\rho_B} \right]. \quad (18)$$

On the left-hand side, we have the difference between the resistivity of the wire and that of the film, which is measured in our experiment. On the right-hand side, the surface-induced resistivities are normalized with respect to the bulk resistivity in order to correspond with the format of the theoretical models. The appropriate theoretical expressions were already given in Eq. (1) for films and in Eqs. (5) and (9) for wires. Knowing the dimensions and the bulk values, the right-hand side of the equation depends only on the specularly parameter. If good fitting to experiment is obtained, this value can be reliably extracted from the results, overcoming the problem of the two parameters fitting. More important than that, good fitting would confirm the theory of surface-induced resistivity for wires with two small dimensions, unlike the case in previous studies where this effect was masked and mixed with that of grain boundaries.

## IV. RESULTS AND DISCUSSION

The experimental data for the resistivity of the films are shown in Fig. 7 both at room temperature and at liquid nitrogen temperature. As expected, an increase in resistivity is observed with the decrease in film thickness. For all films, almost a constant difference between the resistivities in the two temperatures was measured. This is in agreement with our theoretical prediction as for the dependence of resistivity on temperature for thin films,<sup>14</sup> predicting approximately a

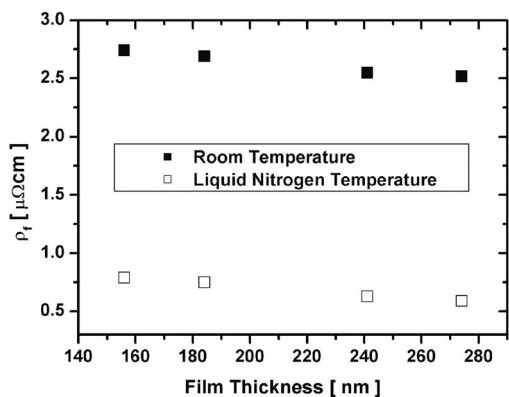


FIG. 7. Experimental data for the resistivity of the films that were used for comparison with the wires. Results are shown for both room and liquid nitrogen temperatures. As expected, an increase in resistivity is observed with decreasing film thickness.

constant slope in these conditions, regardless of the film thickness.

Room temperature measurements of wires with width down to 100 nm showed very similar resistivity values to films with the same vertical dimension. At this temperature, the resistivity increase is dominated by the grain boundary effect with only a small contribution from the surface effect. This result supports our assumption that the difference in the grain boundary effect between the wire and its corresponding film can be neglected for this range of dimensions. As explained by Thompson,<sup>13</sup> it is the vertical dimension that determines the mean grain size in thin films, resulting from energetic and kinetic considerations. Similar arguments are applicable also for wires, provided columnar grain structure is reached with no growth process that is limited by the wire’s sidewalls. Experimental evidence that this is the case in our study was given in Fig. 5. The reason for such structure is probably related to the grain growth during the annealing process that takes place before the excess of copper is removed from top of the trenches. The copper height is not limited then by the trench, enabling a columnar grain structure to be formed, even when the wire’s width is smaller than its height, but still larger than 100 nm. In such a case, no difference is expected between the multidirectional mean grain size in the film and unidirectional mean grain size along the wire, which explains our resistivity results. It should be noted that Steinhogl *et al.*<sup>8</sup> measured a difference of up to 20% between the room temperature resistivity of wires 100 to 800 nm wide (and larger difference for narrower wires). They attributed part of this difference to the grain boundary effect, supporting their claim by showing a decrease in the mean grain size with decreasing width. The difference between their results and ours may be due to their lower annealing temperature that limited the extent of grain growth (175 °C in their case in comparison to 250 °C in ours).

The resistivity of the wires at liquid nitrogen temperature is shown in Fig. 8(a). Each group of wires with a constant height but a variable width is connected with a dotted line. As can be seen, both dimensions affect the resistivity of the wire, which is larger the narrower and the shallower the

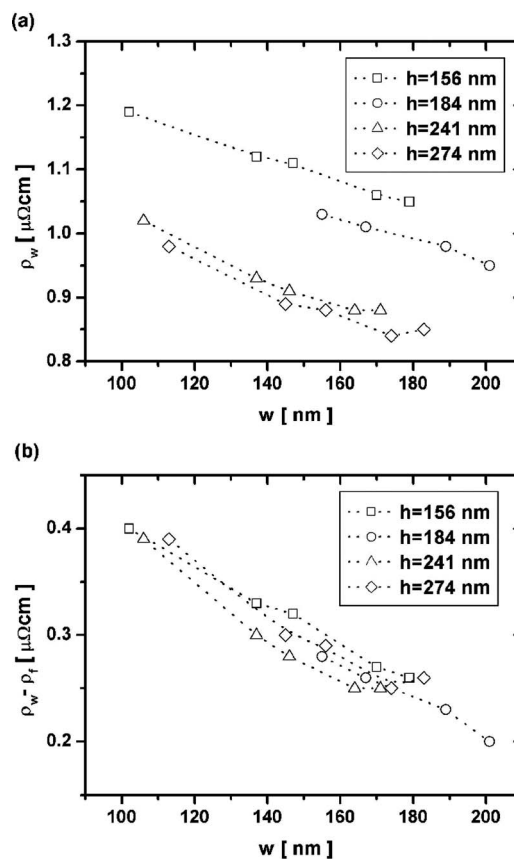


FIG. 8. The resistivity of wires with variable width and height in liquid nitrogen temperature: (a) as measured; and (b) when the resistivity of films with identical vertical dimension is subtracted. Each group of wires having constant height but variable width is connected with a dotted line. The effect of each small dimension and the net contribution of the sidewalls to the resistivity of the wires can be seen.

trench is. As previously demonstrated, separating the contribution of the grain boundaries from that of the surfaces is impossible from these results. In Fig. 8(b), we subtracted from the resistivity of each wire the resistivity of the film with the same vertical dimension (each group of wires has one corresponding film, the resistivity of which was shown in Fig. 7). The result reflects the net surface contribution of the sidewalls to the resistivity of the wires. Surprisingly, all results seem to fall on the same line, implying a separate contribution of each small dimension (filmlike behavior) with no substantial interaction between them. To get a better understanding of this result, the theoretical resistivity of the wire was compared to the expected resistivity in the absence of any interaction between the two dimensions. In this case, the resistivity of the wire can be approximated using Matthiessen’s rule and expressed as

$$\rho_w = \rho_{f(h)} + \rho_{f(w)} - \rho_B, \tag{19}$$

where  $\rho_{f(t)}$  is the resistivity of a film with thickness  $t$ . We will check this approximation only for surface-induced resistivity since the incorporation of the grain boundary effect would only add a constant value. For this case,

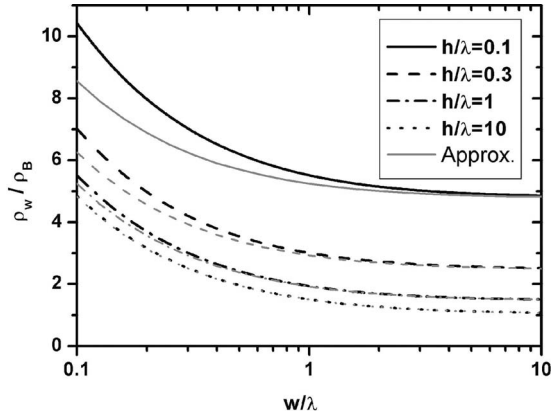


FIG. 9. Comparison between accurate solution (black) and approximation (gray) for the resistivity of a wire with variable width and height. The case of zero specularly parameter ( $p=0$ ) is considered. The approximation neglects the interaction between the width and height of the wire and assumes separate contribution to the resistivity from each small dimension (filmlike behavior).

$$(\rho_s)_w = (\rho_s)_{f(h)} + (\rho_s)_{f(w)} - \rho_B. \quad (20)$$

Figure 9 shows a comparison between the accurate solution and the above approximation. The case of fully diffused scattering ( $p=0$ ) was chosen to estimate the maximal possible deviation. The accurate calculation was identical to the one presented in Fig. 4(a). The approximation in Eq. (20) was calculated using Eq. (1) to express the surface-induced resistivity of the films. As can be seen, the approximation (shown in gray) is good as long as dimensions are not too small in comparison to the mean free path of the electrons. It is valid within 5% accuracy as long as both width and height are larger than one third of the mean free path. All our wires are within this range at liquid nitrogen temperature when the mean free path for copper is about 300 nm, which explains the obtained result.

Substituting this approximation into Eq. (18) further simplifies it to

$$\rho_w - \rho_f = \rho_B \left[ \frac{(\rho_s)_{f(w)}}{\rho_B} - 1 \right]. \quad (21)$$

Comparison to experiment can now be made with only the specularly parameter to be fitted, provided the bulk resistivity and the mean free path are known at the measured temperature. In fact, since the product of the bulk resistivity and the mean free path is constant for all temperatures  $\rho_B \lambda = C$  (free electron approximation), the last equation can be written as

$$\rho_w - \rho_f = \frac{C}{\lambda} \left[ \frac{(\rho_s)_{f(w)}}{\rho_B} - 1 \right]. \quad (22)$$

The advantage of this form is that the expression on the right-hand side depends very weakly on the mean free path, so in addition to the specularly parameter only the constant  $C$  has to be determined for the fitting process. Taking the room temperature values of  $\rho_B = 1.67 \mu\Omega \text{ cm}$  and  $\lambda = 39 \text{ nm}$  for pure copper results in  $C = 6.51 \times 10^{-16} \Omega \text{ m}^2$ . With this

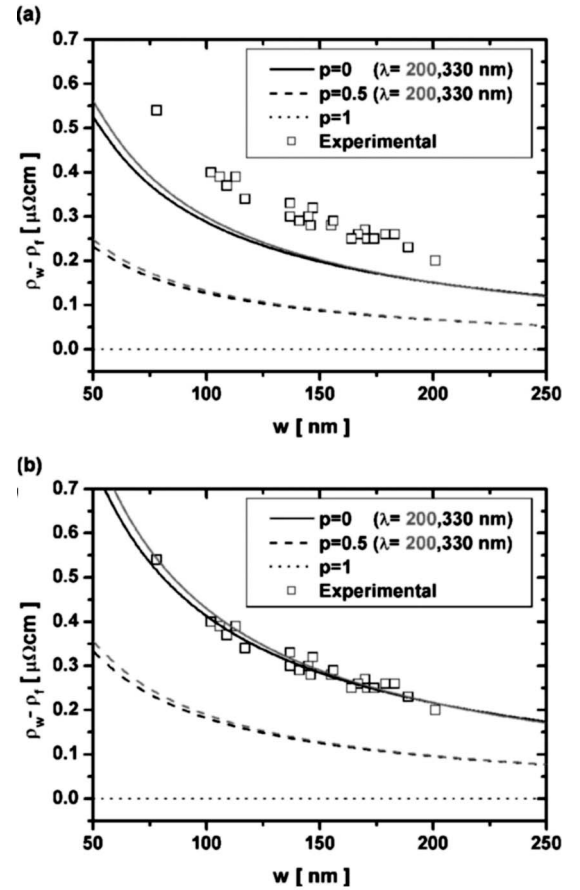


FIG. 10. Fitting theory to the experimental results: (a) assuming the literature value of  $\rho_B = 1.67 \mu\Omega \text{ cm}$  for the room temperature bulk resistivity and (b) taking the estimated value for our case of  $\rho_B = 2.30 \mu\Omega \text{ cm}$ . The weak dependence on the mean free path value at liquid nitrogen temperature is demonstrated by choosing two extreme values of 200 nm (gray) and 330 nm (black). Best fit is obtained for zero specularly parameter.

value the fit to experimental results is shown in Fig. 10(a). The experimental data from the special set of wires shown in Fig. 3 was also included this time (height of this set was 96 nm and the measured resistivity of its film was  $3.17 \mu\Omega \text{ cm}$  at room temperature and  $1.13 \mu\Omega \text{ cm}$  at liquid nitrogen). The very weak dependence on the mean free path value is demonstrated by choosing two extreme values of 200 and 330 nm for it at liquid nitrogen temperature (the last is the tabulated value used in Ref. 7). As can be seen, the fit to experimental results is closest for a zero specularly parameter, but the predicted values are still low in comparison to the measured ones. We attribute this difference to the bulk resistivity, which is higher in our case than the literature value for macroscopic copper conductors. This is due to the process of electrochemical deposition that incorporates impurities and other defects that increase the background scattering within the grains. Higher bulk resistivities were also obtained by Steinhogel *et al.*<sup>7,8</sup>

We can estimate the bulk resistivity from the films measurements shown in Fig. 7. It is certainly less than  $2.52 \mu\Omega \text{ cm}$  which is the resistivity of thickest film (274 nm). An asymptotic value of  $\rho_B = 2.30 \mu\Omega \text{ cm}$  seems as a good ap-

proximation. With this value excellent agreement with the experimental results is obtained for zero specularly parameter, as shown in Fig. 10(b) (changing the value of the bulk resistivity in the allowed range results in a very similar conclusion with near zero specularly parameter). The presented theory of surface-induced resistivity in wires is thus confirmed and meaningful extraction of the specularly parameter is enabled. The low value obtained for this parameter emphasizes the importance of surface scattering to the resistivity increase of nanometric wires.

## V. SUMMARY

Comparing the resistivity of wires to that of films with identical vertical dimension was shown to be very useful for studying their surface-induced resistivity. The suggested model enabled us to separate the contribution of surfaces from that of grain boundaries and extract meaningful parameters from the experimental results. When both width and height of the wire are larger than one third of the mean free path of the electrons, the wire exhibits filmlike behavior with separate contribution to the resistivity from each small dimension. Matthiessen's rule can then be applied to calculate the resistivity of the wire from the known expressions for the resistivity of thin films. Zero specularly parameter best described the scattering of the copper electrons at their interfaces with the surrounding tantalum layer. It means a very strong surface effect that must be taken into account. It is left for further investigation to try to understand the obtained specularly parameter on the basis of the interface properties. The presented approach enables such an investigation and it would be especially interesting to predict and test whether another material in the interface (titanium, for example) would result in a different specularly parameter.

## ACKNOWLEDGMENTS

This work was supported by the Magnet Program of the Chief Scientist Office at the Israeli Ministry of Industry and Trade, Consortium of Emerging Dielectric and Conductor Technologies for the Semiconductor Industry. H. Marom acknowledges the support of an Israel Ministry of Science Es-khol grant.

## APPENDIX

Chambers<sup>11</sup> developed the following expression for the resistivity of a wire with general cross section ( $\rho_w$ ) that is higher than that of a bulk material ( $\rho_B$ ) due to fully diffuse scattering at the wire's walls ( $p=0$ ):

$$\frac{\rho_B}{\rho_w} = 1 - \frac{3}{4\pi s} \int_s \int_0^{2\pi} d\phi \int_0^\pi d\theta \sin \theta \cos^2 \theta \exp\left(-\frac{OP}{\lambda}\right), \quad (\text{A1})$$

where  $s$  is the cross section of the wire in the  $xy$  plane,  $O$  is some point inside the wire,  $P$  is some point on its surface,  $OP$  is the distance between  $O$  and  $P$ ,  $\theta$  is the angle between

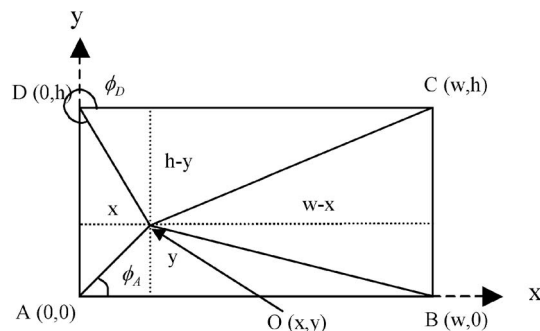


FIG. 11. Using Chambers's approach to calculate the surface-induced resistivity of a rectangular wire (see Appendix for further details).

the vector  $PO$  and the  $z$  axis, and  $\phi$  is the azimuthal angle of  $PO$  around the  $z$  axis. For a wire with a rectangular cross section (width  $w$  and height  $h$ ), this expression becomes

$$\frac{\rho_B}{\rho_w} = 1 - \frac{3}{4\pi h w} I, \quad (\text{A2})$$

where

$$I = \int_0^w dx \int_0^h dy \int_0^{2\pi} d\phi \int_0^\pi d\theta \sin \theta \cos^2 \theta \exp\left(-\frac{OP}{\lambda}\right). \quad (\text{A3})$$

To calculate the resistivity, one has to express  $OP$  in terms of the angles  $\theta$  and  $\phi$  and then conduct the integration. Since  $\theta$  is the angle between  $PO$  and the  $z$  axis, then  $OP = OP_{xy}/\sin \theta$ , where  $OP_{xy}$  is the projection of  $OP$  on the  $xy$  plane. This projection is shown in Fig. 11. Point  $O$  has general coordinates  $(x,y)$  and point  $P$  is anywhere on the surface, including the marked points in the corners. It is convenient to split the integral  $I$  to the four segments and treat each segment separately. Thus  $I = I_{AB} + I_{BC} + I_{CD} + I_{DA}$ ; since it is clear that  $I_{AB} = I_{CD}$  and  $I_{BC} = I_{DA}$ , we can write  $I = 2(I_{AB} + I_{DA})$ . Focusing on the  $DA$  segment, it is easy to verify that for all points on this surface  $OP_{xy} = x/\cos \phi$ . The integration over  $\phi$  should be performed from  $\phi_D$  to  $\phi_A$  (see Fig. 11) that can be found from the geometry of the problem (note that  $\phi$  is defined by the direction  $PO$  and is measured with respect to the  $x$  axis):  $\phi_A = \arctan(y/x)$  and  $\phi_D = \arctan[(y-h)/x]$ . We can therefore write

$$I_{DA} = \int_0^w dx \int_0^h dy \int_{\arctan[(y-h)/x]}^{\arctan(y/x)} d\phi \int_0^\pi d\theta \sin \theta \cos^2 \theta \times \exp\left(-\frac{x}{\lambda \sin \theta \cos \phi}\right). \quad (\text{A4})$$

A similar analysis can be used to find  $I_{AB}$  but it is easier to take advantage of the symmetry of the problem and deduce

$I_{AB}$  from  $I_{DA}$  simply by replacing each  $x$  with  $y$  (and vice versa) and each  $h$  with  $w$  (and vice versa). Thus,

$$I_{AB} = \int_0^w dx \int_0^h dy \int_{\arctan[(x-w)/y]}^{\arctan(x/y)} d\phi \int_0^\pi d\theta \sin \theta \cos^2 \theta \times \exp\left(-\frac{y}{\lambda \sin \theta \cos \phi}\right). \quad (\text{A5})$$

Using the above expressions for  $I_{AB}$  and  $I_{DA}$ , the resistivity of the wire in the case of fully diffuse scattering ( $p=0$ ) can be written as

$$\frac{\rho_B}{\rho_w} = 1 - \frac{3}{2\pi h w} (I_{DA} + I_{AB}). \quad (\text{A6})$$

\*Electronic mail: hagaym@tx.technion.ac.il

<sup>1</sup>K. Fuchs, Proc. Cambridge Philos. Soc. **34**, 110 (1938).

<sup>2</sup>A. F. Mayadas and M. Shatzkes, Phys. Rev. B **1**, 1382 (1970).

<sup>3</sup>H. D. Liu, Y. P. Zhao, G. Ramanath, S. P. Murarka, and G. C. Wang, Thin Solid Films **384**, 151 (2001).

<sup>4</sup>J. W. Lim, K. Mimura, and M. Isshiki, Appl. Surf. Sci. **217**, 95 (2003).

<sup>5</sup>W. Wu, S. H. Brongersma, M. Van Hove, and K. Maex, Appl. Phys. Lett. **84**, 2838 (2004).

<sup>6</sup>C. Durkan and M. E. Welland, Phys. Rev. B **61**, 14215 (2000).

<sup>7</sup>W. Steinhogel, G. Schindler, G. Steinlesberger, and M. Engelhardt,

Phys. Rev. B **66**, 075414 (2002).

<sup>8</sup>W. Steinhogel, G. Schindler, G. Steinlesberger, M. Traving, and M. Engelhardt, J. Appl. Phys. **97**, 23706 (2005).

<sup>9</sup>D. K. C MacDonald and K. Sarginson, Proc. R. Soc. London, Ser. A **203**, 223 (1950).

<sup>10</sup>R. B. Dingle, Proc. R. Soc. London, Ser. A **201**, 545 (1950).

<sup>11</sup>R. G. Cambers, Proc. R. Soc. London, Ser. A **202**, 378 (1950).

<sup>12</sup>H. Marom, M. Ritterband, and M. Eizenberg, Thin Solid Films **510**, 62 (2006).

<sup>13</sup>C. V. Thompson, Annu. Rev. Mater. Sci. **20**, 245 (1990).

<sup>14</sup>H. Marom and M. Eizenberg, J. Appl. Phys. **96**, 3319 (2004).